JOURNAL OF CRITICAL REVIEWS

ISSN- 2394-5125 VOL 6, ISSUE 07, 2019

An AI-Powered Automatic Lane-Line Detection System

[1]JOGU PRAVEEN, M.Tech Assistant Professor, jpraveen.pec@gmail.com
[2]CHEEKATYALA ANJAN KUMAR ,M.Tech Assistant Professor , anjankumarcheekatla@gmail.com
Department-ECE
Nagole Univerisity Engineering and Technology Hyderabad

ABSTRACT

Recently, lane line detection has received a lot of attention due to the increasing need for an intelligent transportation system. A lane line detection approach for bettering the YOLOv3 network structure is provided as a solution to the issue of the YOLOv3 algorithm's poor accuracy and high likelihood of missed detection while identifying lane lines in complicated surroundings. The change is an concentration on rapid and precise detection. First, the lane line photographs are separated into s 2S grids based on the pictures' inconsistencies in vertical and horizontal distribution density.

Introduction

Trace monitoring and autonomous vehicles are two examples of intelligent transportation systems in which lane line detection plays a crucial role [1]. Consequently, there is a growing need for lane line detecting systems [2]. Ways to identify lanes have been explored in a number of different ways. Generally speaking, these strategies may be broken down into two categories: classifications: conventional approaches and those based on deep learning methods. The statistical technique is the basis of conventional isolating characteristics of images [3] Color, grayscale, and edge detection are only a few examples. However, deep learning-based methods rely on feature extraction using convolutional neural networks [4]. It's true that conventional methods may often provide accurate results, Ideally, the conventional method requires method that is both labor-intensive and intricate. process of creating and releasing software [5]. Furthermore, However, the training cannot be disseminated via conventional methods. a response from its feature extractor [6] section. Consequently, this strategy is seen as harmful to manufacturing output. inserting these questions with the help of deep learning is difficulty with the conventional method. For example, a major challenge in creating a deep learning model is the compromise between precision and efficiency. rapidity with which the model is detected. Very precise models often need elaborate feature extraction, causes a slow rate of detection. Therefore, it's crucial to provide a solid foundation. both of these considerations must be taken into account while designing learning models aspects.

Related Work

The three most common approaches to lane line identification today are road feature extraction using machine vision, road model establishment, and lane line detection using a human. multi-sensor fusion detection technique [9]. The machine-extraction technique for road characteristics vision relies heavily on automated categorization tools provided by machine characteristics of lane lines' grayscale values and colours. After road's lane lines using just machine learning. Because grayscale, colour, and other image characteristics are often environmental factors, such as light levels and shadow; detecting lane lines with this technique is simple. be unsettled by changes in the surroundings [10]. procedure for determining the detecting road model consists of putting down roots in either the 2D or 3D road picture using a computerised tomography model, and then contrasting the result with the original photo's lane line that has to be identified. the application This technique of detection has a limited scope, and it is restricted to streets of a certain identified kind templates. Furthermore, the algorithm stores a great deal data calculations, and subpar response time in the actual world .To begin processing a picture, the algorithm segments it into ss grids. If the target's geometric centre coincides with a grid's detection area, then the grid is responsible for the detection. It's a lot of The expected parameters for each grid are shown in the subsequent formula

$$\text{Num} = s * s(5 * B + C). \qquad (1)$$

If you look at the first formula, B is the total number of boundary boxes, and C is the total number of class probabilities [16]. Five expected values (in X, Y, W, and H dimensions) make up each box. Each bounding box has a confidence value, denoted by the symbol "conf. Abscissa (X) and ordinate (Y) stand for two different dimensions. location of the box's pivot point in coordinate space, where the width and height are the values W and H, respectively. limits of a space.

the degree to which each respective confidence interval The target is within the boundary, and the precision of its foresight. You can see how confidence is defined in the formula below:

$$\text{Conf} = \Pr(\text{Object}) \times \text{IoU}(\text{Pred}, \text{Truth}). \qquad (2)$$

$$\text{IoU}(\text{Pred}, \text{Truth}) = \frac{\text{area}(\text{Boxt} \cap \text{Boxp})}{\text{area}(\text{Box} \cup \text{Boxp})}. \qquad (3)$$

Pr (Class I | Object) is the conditional category probability in formula (4), which assumes that the grid includes detection targets and that each of those targets is an object. grid only forecasts the likelihood of one kind of event: purposes [18]. The probability that a given class is detected, denoted by Pr (Class I target refers to an instance of the class target [19].

$$\Pr(\text{Class } i \mid \text{Object}) = \frac{\Pr(\text{Class } i)}{\Pr(\text{Object})}. \qquad (4)$$

These are the primary distinctions between YOLOv3 and its predecessors:

employing the core network concept of darknet-53 (106 layers overall, including 53 convolution layers); using decentralized inference classifier in place of the softmax function, and employing a technique very much like FPN for predicting features at several scales. The original YOLOv2 only supports 1 convolution. while using a single feature map and a detection kernel. -e most notable YOLOv3's tri-size target detection capability is a notable improvement. Larger objects may be detected when the feature size is 13. Objects; if the feature size is 26 by 26, it may be utilised to targets of medium size; when the feature size is 52 by 52 used to identify tiny targets. Consequently, it is a solution to the challenge of fine-tuning the surveillance system to account for proportionality to the target's size [21].

ISSN- 2394-5125 VOL 6, ISSUE 07, 2019

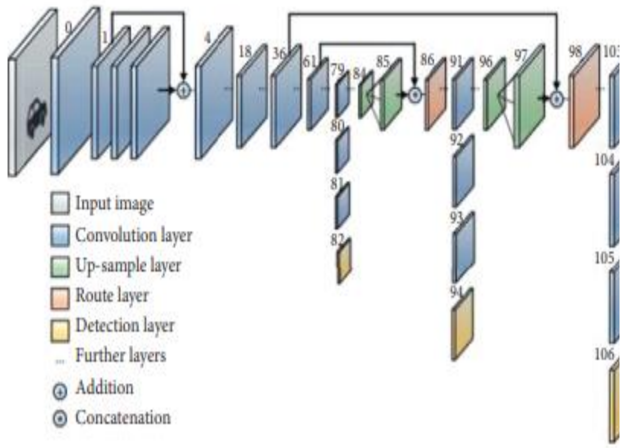

Figure 1: Network structure model of YOLOv3

Three feature maps of varying sizes are used in YOLOv3, and their respective detection steps are 32, 16, and 8. Layer 82 of the darknet-53 network is where the first detection layer may be found for 416 x 416 pixel images. In light of the fact that its detection stage is Resolution of this layer's feature map is 32. layers of 13 second layer of detection is found in the layer Network node 94 on the dark web 53. Due to the fact that its detecting step is 16, Its feature map is a high-resolution image, measuring 26 third layer of detection is found at layer 106 of The 53rd Dark Web Network An 8-step detection process is necessary for The feature map for this layer is a high-resolution image, measuring in at 52 ∗ 52 [22].

$$L = L_{\text{coord}} + L_{\text{conf}} + L_{\text{class}}. \tag{5}$$

The formula for Cord is presented below (6). The formula's chord term stands for the coordinate error weighting coefficient, S2 for the squared number of grids, and so on. image, and B stands for some bounded number of predictions. grid's individual boxes is shorthand for the chance that the target items are located in the I-th grid's prediction box. If Aims Are Met included, 1; not included, 0 (xi, yi, wi, hi), gives you the values for the abscissa, ordinate, width, and height of the actual bounding box's (BB's) centre in the i-th grid [24].

$$L_{\text{coord}} = \lambda_{\text{coord}} \sum_{i=0}^{S^2} \sum_{j=0}^{B} I_{ij}^{\text{obj}} \left[(x_i - \hat{x}_i)^2 + (y_i - \hat{y}_i)^2 + w_i - \hat{w}_i + \left(h_i - \hat{h}_i\right)^2 \right]. \tag{6}$$

The I-th grid's jth prediction box does not have any targets. Constants in the formula have the same meaning as in

$$L_{\text{Conf}} = \sum_{i=0}^{S^2} \sum_{j=0}^{B} I_{ij}^{\text{obj}} \left[\left(C_i - \hat{C}_i\right)^2 \right] + \lambda_{\text{noobj}} \sum_{i=0}^{S^2} \sum_{j=0}^{B} L_{ij}^{\text{noobj}} \left[\left(C_i - \hat{C}_i\right)^2 \right]. \tag{7}$$

The formula defining Class is shown (8). -ere are C different kinds of targets to be found (c 1, 2, 3,..., C), and, Probabilities that are genuine and those that are predicted targets belonging to the cth class in the ith grid. Any additional numbers used in the formula have the same significance as number 6

$$L_{\text{class}} = \sum_{i=0}^{S^2} I_{ij}^{\text{obj}} \sum_{c \in \text{class}} \left[\left(P_i(C) - \hat{P}_i(C) \right) \right]^2. \tag{8}$$

Proposed Method

The YOLOv3 technique is often used for real-time target recognition, however it is susceptible to interference from environmental conditions including lighting and ground dampness. so forth. To enhance the precision and speed of detection,bIn this study, we refine the YOLOv3 algorithm, making it more suited for lane line recognition. System nModifications Made to the Core 3.1. To begin, Darknet-53 serves as the foundation of the standard YOLOv3 algorithm. to which the input picture is similarly segmented into s s grids. When For lane line detection, The longitudinal axis is a distinguishing characteristic of lane line images. proportionally longer than its transverse counterpart. Consequently, higher grid detection densities are needed. using a longitudinal picture, the method is enhanced by slicing the picture into 2S by s grids The lane-line network is a better suited structure. a method of detecting something.

$$D = \min \sum_{\text{box}=0}^{n} \sum_{\text{cen}=0}^{k} [1 - \text{IoU}]. \quad (9)$$

Table 1 displays the results of a comparison between the upgraded approach and the original YOLOv3 algorithm for detection. Its average precision and velocity surpass those of algorithmic predecessor to YOLOv3. This demonstrates that the enhanced technique for determining the anchor settings is more appropriate for picking up subtle targets like lane lines. Loss Function, as described in Section 3.3. The -e loss function is used in the estimation of deviation from the expected value to the actual value using the model that provides the framework for assessing the validity of the false rate of detection by the neural network, which represents the network model's convergence performance. -e loss The YOLOv3 algorithm's function is broken down into three distinct sections: shown by the formula (5).

$$f(x) = \frac{1}{1 + e^{x}}, \quad (10)$$

$$f'(x) = \frac{e^{x}}{2e^{x} + e^{2x} + e^{2x}(1/e^{x})^{2}}. \quad (11)$$

Logistic functions are single and continuous, with a finite range of possible values. So, the

During transport via a network, information will not change. - The derivative of this function has a value smaller than 1, which is a defining property of the derivative. Network input value is mistake in calculating the derivative will be negligibly high if the original error is As the loss function is increased in size, the network model's convergence performance will improve worse. To address the aforementioned issues, focus loss in place of the logistic function in the algorithmic novelty. -e analytic formulation of the focused loss function and the formula proves it (12). The result, denoted by p in formula (12), proportional value (1 p) to the logistic function Adjustment factor target node's weight coefficient in the network system's category (-1 to 1), c the focusing coefficient (c 0), and y the anticipated probability value of the tag.

$$\text{FL}(p, y) = -\alpha y (1 - p)^{\gamma} \lg p - (1 - \alpha)(1 - y) p^{\gamma} \lg (1 - p), \quad (12)$$

$$L_{\text{coord}} = \lambda_{\text{coord}} \sum_{i=0}^{S^2} \sum_{j=0}^{B} I_{ij}^{\text{obj}} \left[\text{FL}(x_i, \hat{x}_j) + \text{FL}(y_i, \hat{y}_j) \right] + \lambda_{\text{coord}} \sum_{i=0}^{S^2} \sum_{j=0}^{B} I_{ij}^{\text{obj}} \left[\text{FL}(w_i, \hat{w}_j) + \text{FL}(h_i, \hat{h}_j) \right], \quad (13)$$

$$L_{\text{conf}} = \sum_{i=0}^{S^2} \sum_{j=o}^{B} I_{ij}^{\text{obj}} \left[\text{FL}(C_i, \hat{C}_j) \right] + \lambda_{\text{noobj}} \sum_{i=0}^{S^2} \sum_{j=o}^{B} I_{ij}^{\text{noobj}} \left[\text{FL}(C_i, \hat{C}_j) \right], \quad (14)$$

$$L_{\text{class}} = \sum_{i=0}^{S^2} I_{ij}^{\text{obj}} \sum_{c=\text{class}}^{S^2} \left[\text{FL}(P_i(C), \hat{P}_i(C)) \right]. \quad (15)$$

ISSN- 2394-5125 VOL 6, ISSUE 07, 2019

The enhanced loss function's target classification prediction error, error in predicting the coordinates of boundary boxes, and error in predicting the confidence of boundary box predictions are shown in 13-15, in order. Incorporating the new, more effective adjustment factor, the limited-coverage reception area has Targets like lane line are easier to hit and The reliability of detection has increased.

a technology that can automatically identify lane lines. The lane line detection system's primary components are the data preparation module, the learning and training module, and the lane line detection module, all of which are based on the enhanced YOLOv3 algorithm network structure. modules for detection, and the steps involved in their implementation are detailed in See also: Figure The meat and potatoes of the data prep module are the Accumulating, Tabbing, Sifting, and Preprocessing Lane Installing a line sampler is the most common technique of collecting samples from a production attach a high-resolution camera to the vehicle and snap pictures of the road markings. going toward; en route. The term "data marking" describes the practise of clearly image, complete with yellow highlights, white dots, and white solid lines.

$$t(x', y') = s(\mathrm{int}(x + 0.5), \mathrm{int}(y + 0.5)). \qquad (16)$$

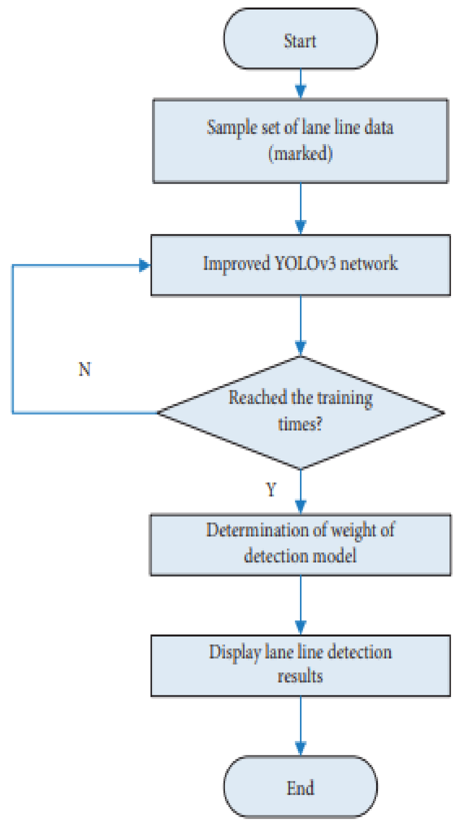

Figure 3: Process of the lane line detection system

ISSN- 2394-5125 VOL 6, ISSUE 07, 2019

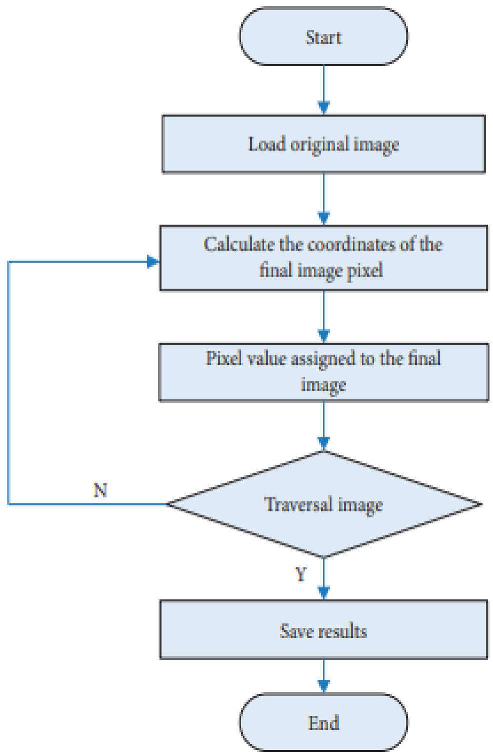

Figure 4: Flow chart of the nearest neighbor down sampling algorithm

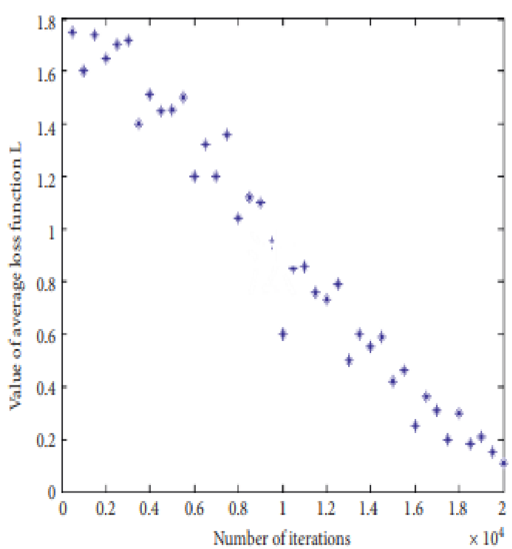

Figure 5: Variation trend of average loss function value.

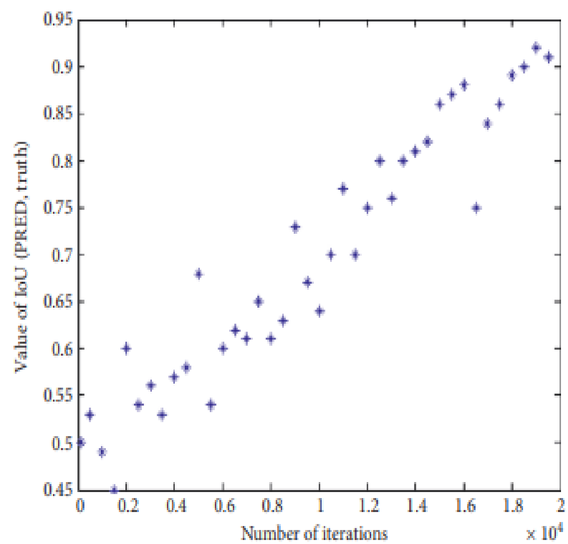

Figure 6: Change trend of matching degree value.

Results and Discussion

Setup for Scientific Experimentation. CPU (Intel® CoreTM-i7 4720HQ, 2.6 GHz) and GPU (NVIDIA TITAN X, 12 GB VRAM) hardware was employed in the experiment. equivalent hardware environment OS Ubuntu. Data set used in the 4.2 Experimental Phase. KIW - Karlsruhe Institute of Technology The Kyoto Institute of Technology and Design (KITTI) is an established Japanese institution of utilised traffic data set that include settings like sunny, overcast, and others. Captivating experiences are intensified under the influence of challenging circumstances, including wet, tunnel, and at the end of the day or at night to make sure everyone is covered. KITTI is used here as a collected information, or data set. Five hundred pictures of city streets were chosen: four hundred for

ISSN- 2394-5125 VOL 6, ISSUE 07, 2019

training and one hundred for testing. Experimental Findings and Analyses. There is a well delineated lane dividing traffic. The enhanced YOLOv3 algorithm network is trained using images received from the training process. The magnitude of the training phase the standard for these images is 416 by 416. While learning new skills, There are a number of crucial index factors in the method, including captured on the fly. Average loss function evolution As for the L-value, it is shown in Figure 5. Figure 5 demonstrates that at the time Loss function value is around 1.8 at the start of training. Convergence of rises as the number of training grows. The value of the loss function drops. If you run the algorithm for 20,000 times, you'll get a loss of just approximately 0.1. The intended result of using function L has been attained.

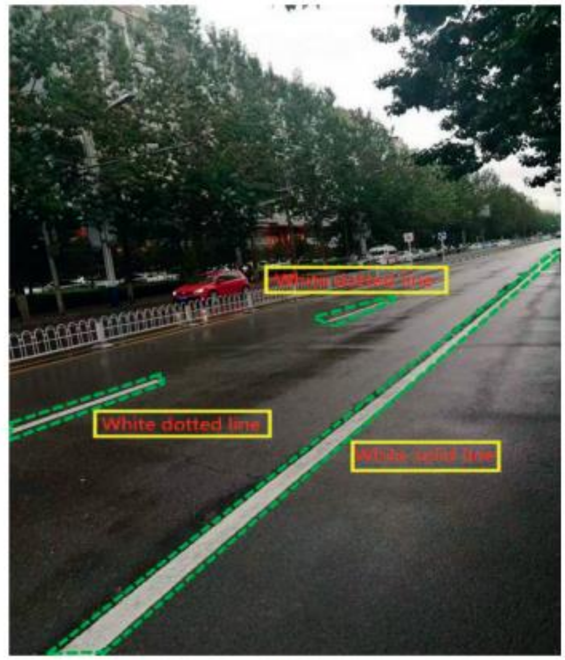

(b)

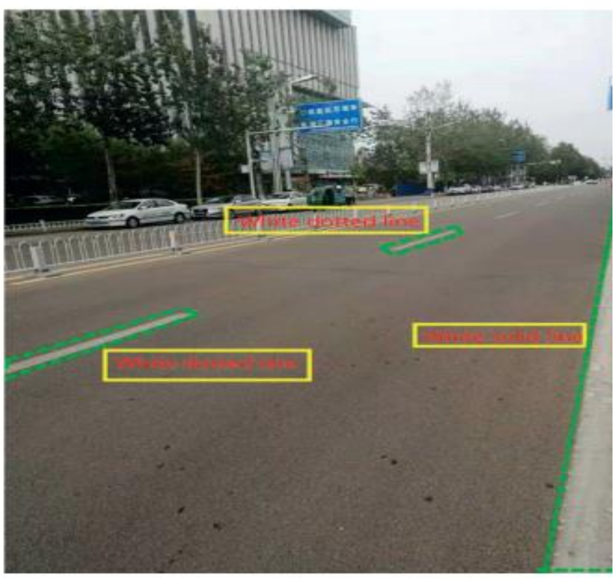

(a)

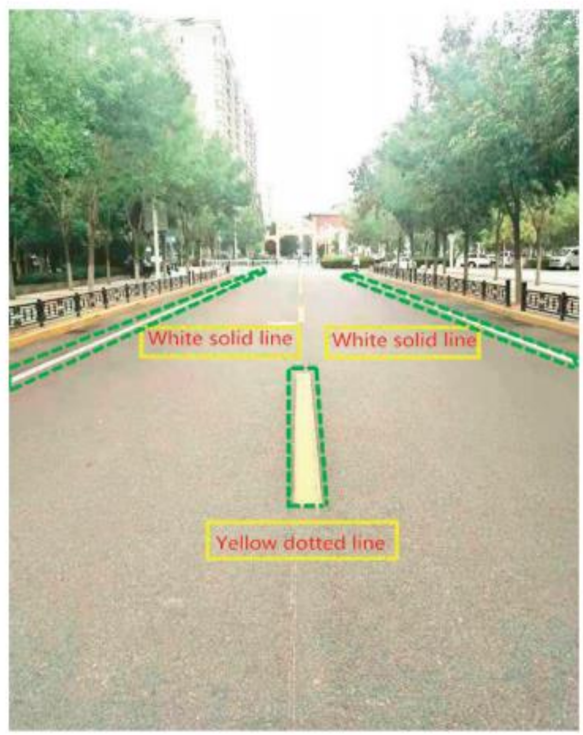

(c)

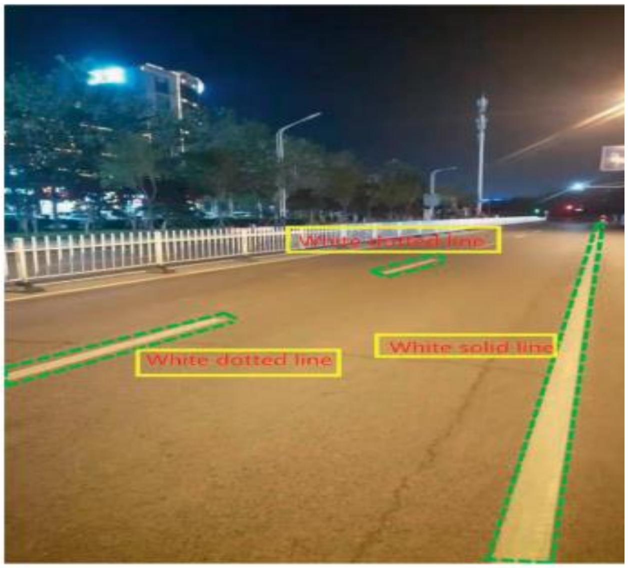

(d)

Figure 7: Results in difference scenes: (a) normal illumination; (b) rainy days; (c) bright light; (d) dark light at night.

After 20000 rounds, the IoU (Pred, Truth) value is around 0.93, indicating that the -e detection accuracy has produced the desired result. The average loss function L, which is given a factors include IoU (Pred, Truth), the training We've decided to run the model for 20000 iterations. Once the demo has been mastered one hundred pictures of lane lines are used for testing and training the system. can analyse images and detect lane lines automatically. Results from the system's testing in a variety of settings are shown in Pictured here is Figure 7. Examining Alternative Algorithms (4.4) Fast Track Automatic Lane The YOLOv3 enhancements provide for an effective line detecting system. accuracy, detection time, and number of false positives and negatives rate of detection, and so forth. e Key Performance Indicators of

Table 2: Comparison of test performance of difference algorithms

Algorithm	FPS	mAP (%)	Times of iterations when $L = 0.1$	Average missed detection rate (%)
YOLO v3	8	84.87	20922	2.4
R-CNN	6	87.35	22178	4.2
Fast R-CNN	10	86.27	21896	8.1
Faster R-CNN	11	80.73	19989	9.3
YOLOP	11	81.04	20012	4.9
Improved YOLOv3	12	91.03	19985	1.1

Algorithms of many types are shown in Table 2. In comparison to previous versions of YOLO, the new and upgraded YOLOv3 model clearly performs better in terms of its lane line identification mechanism. Everything is an algorithm.

Conclusion

A detection method based on the enhanced YOLOv3 aims to solve the issue of standard lane detection algorithms being unable to strike a compromise between detection accuracy and detection speed. This study suggests a new algorithm. The most significant changes are First, in keeping with the features of inconsistent density of lanes both vertically and horizontally pictures into horizontal and vertical line images is suggested. Increase the vertical detection density using s 2S grids. The e-detection scale has been set to a detection level of 4. measurements on the 13 13, 26 26, 52 52, and 104 104 scales, enables more precise recognition of low-volume objects like highway markings To wit: The framework of YOLOv3 has been altered by including The simplified network and increased system performance provided by Darknet-49's design. Fourth-order e parameters include things like cluster centre distance and Incorporating enhancements to the loss function makes the algorithm more applicable to use with a technology that can

ISSN- 2394-5125 VOL 6, ISSUE 07, 2019

identify lines delineating lanes The revised algorithm has high detection performance for identifying flat surfaces, as shown by the experiments. highways, however, when the roads have steep inclines, detection is simple to influence. Therefore, addressing the lane issue The main emphasis of the next section will be line identification in scenarios with a lot of slope. study of the topic more thoroughly.

References

[1] H. G. Zhu, "An coefficient lane line detection method based on computer vision," Journal of Physics: Conference Series, vol. 1802, Article ID 032006, 2020.

[2] R Mia, Y. Chen, and B. Ren, "Improved anti-occlusion object tracking algorithm using unscented rauch-tung-striebel smoother and kernel correlation filler," Journal of King Saud University - Computer and Information Sciences, vol. 18, no. 3, pp. 22–30, 2022.

[3] C. Y. Fu, W. Liu, and A. Ranga, "Deconvolutional single shot detector," 2021, https://arxiv.org/abs/1701.06659.

[4] T. Lin, P. Doll ar, R. B. Girshick, K. He, B. Hariharan, and S. J. Belongie, "Feature pyramid networks for object detec tion," in Proceedings of the 2017 IEEE Conference on Computer Vision and Pattern Recognition (CVPR), pp. 936–944, Hon olulu, HI, USA, July 2021.

[5] S. Lee, J. Kim, and I. S. Kweon, "VPGNet: vanishing point guide network for lane and road marking detection and recognition," in Proceedings of the International Conference on Computer Vision, pp. 2380–7504, Venice, Italy, March 2021.

[6] A. Gupta and A. Choudhary, "A framework for camera-based real-time lane and road surface marking detection and rec ognition," IEEE Transactions on Intelligent Vehicles, vol. 3, no. 4, pp. 476–485, 2018.

[7] T. Lin, M. Maire, S. J. Belongie et al., Microsoft Coco: Common Objects In Context" (Eccv), Springer, Berlin, Germany, 2019.

[8] R. B. Girshick, "Fast RCNN," in Proceedings of the 2015 IEEE International Conference on Computer Vision (ICCV), pp. 1440–1448, Washington, DC, USA, December 2020.